determination of the title compound.

Registry No. $[Fe(C_5H_5)(CO)_2(PPh\text{-}t\text{-}BuCl)]PF_6$, 76498-86-7; $[Fe(C_5H_5)(CO)_2(PPh\text{-}t\text{-}BuCl)]BF_4$, 76498-87-8; $[Fe(C_5H_5)(CO)_2(PPh\text{-}t\text{-}BuCl)]BPh_4$, 76498-88-9; $[\{Fe(C_5H_5)(CO)_2(PPh\text{-}t\text{-}BuO)\}_2H]PF_6$, 76498-90-3; $[\{Fe(C_5H_5)(CO)_2(PPh\text{-}t\text{-}BuO)\}_2H]BF_4$, 76498-91-4; $[\{Fe(C_5H_5)(CO)_2(PPh\text{-}t\text{-}BuO)\}_2H]BPh_4$, 76498-92-5; $[Fe(C_5H_5)(CO)_2(PPh\text{-}t\text{-}BuOH)]Br$, 76498-93-6; $[Fe(C_5H_5)(CO)_2(PPh\text{-}t\text{-}BuOHNEt_3)]PF_6$, 76498-94-7; $Fe(C_5H_5)(CO)_2(PPh\text{-}t\text{-}BuO)$, 76498-89-0; $[Fe(C_5H_5)(CO)_2(PPh_2OMe)]I$, 76498-95-8; $[Fe(C_5H_5)(CO)_2(PPh_2OMe)]PF_6$, 76498-97-0; $[Fe(C_5H_5)(CO)_2(PPh_2Cl)]Cl$, 76498-98-1; $[Fe(C_5H_5)(CO)_2(PPh_2Cl)]PF_6$, 76499-00-8; $[Fe(C_5H_5)(CO)_2(PPh_2Cl)]BF_4$, 76499-01-9; $[\{Fe(C_5H_5)(CO)_2(PPh_2O)\}_2H]BF_4$, 76499-03-1; $Fe(C_5H_5)(CO)_2(PPh_2O)$, 76499-02-0; $[Fe(C_5H_5)(CO)_2(PPh_2OH)]Br$, 76499-04-2; $Fe(C_5H_5)(CO)_2Cl$, 12107-04-9; $[Fe(C_5H_5)(CO)_2(THF)]BF_4$, 63313-71-3; $Fe(C_5H_5)(CO)_2I$, 12078-28-3.

Supplementary Material Available: Listing of structure factor amplitudes (6 pages). Ordering information is given on any current masthead page.

Contribution from the Department of Chemistry,
University of Victoria, Victoria, British Columbia, Canada V8W 2Y2

Cationic Pyrazole Complexes of Palladium and Platinum. Characterization of Dynamic Stereochemistry by ^1H and ^{31}P NMR and the Crystal and Molecular Structure of *cis*-Chlorobis(triethylphosphine)(3,5-dimethylpyrazole)palladium(II) Tetrafluoroborate

GORDON W. BUSHNELL, KEITH R. DIXON,* DONALD T. EADIE, and STEPHEN R. STOBART

Received September 11, 1980

Synthesis of the complex cations *cis*-$[MCl(PEt_3)_2L]^+$, M = Pd or Pt, L = pyrazole (pzH), 3,5-dimethylpyrazole (3,5-DMP), 3,4,5-trimethylpyrazole (3,4,5-TMP), or 4-bromo-3,5-dimethylpyrazole (Br-3,5-DMP), is reported. In solution at ambient temperatures, the platinum complexes are static on the NMR time scale but the palladium compounds exhibit rapid averaging of the two nonequivalent phosphorus nuclei and of the 3,5 proton or methyl positions on the pyrazole ligands. Detailed study of the M = Pd, L = Br-3,5-DMP derivative suggests pyrazole dissociation as the rate-determining step in the phosphorus averaging. The mechanism of 3,5-methyl averaging is less clearly established but may involve deprotonation followed by an intramolecular, metallotropic, 1,2 (equivalent to 1,5) shift. X-ray diffraction study of the M = Pd, L = 3,5-DMP cation as its BF_4^- salt shows approximately square-planar coordination with a monodentate 3,5-DMP ligand. Both nitrogen atoms are displaced to the same side of the basic coordination plane by an important hydrogen bond from N(2), which bears the proton, to F(2) in the anion. The Pd atom is significantly displaced (0.348 Å) from the plane of the 3,5-DMP ligand, an effect probably caused by steric interaction of the pyrazole with a PEt_3 ligand.

Introduction

Fluxional processes involving metal transfer between two nitrogen donor sites on an organic ring have been of recent interest to coordination chemists from two points of view. First, the observation of such processes in imidazole complexes of metalloporphyrins has been considered important for its potential biochemical significance.[1] Second, a relationship has been suggested[2] between a 1,2 metal-transfer process between adjacent nitrogen sites in 1-metallopyrazolyls and the well-established fluxional character of (η^1-cyclopentadienyl)metal complexes. That the latter are fluxional by virtue of a 1,5 (equivalent to 1,2) shift, with 1,3 shifts being forbidden, has been substantiated by recent work in these laboratories.[3]

We became interested in these processes through our previous demonstration that phenanthroline in the complex cation *cis*-$[PtCl(PEt_3)_2(phen)]^+$ is essentially monodentate and fluxional by virtue of a metal transfer between the nitrogen donor sites[4] and our extension of these studies to naphthyridine[5] and phthalazine[6] complexes and to palladium.[7] Pyrazole complexes, however, present a different situation in that a proton transfer is necessary in addition to the metal exchange between nitrogen sites, and if the ring exhibits any significant double-bond localization, then electron reorganization will also be necessary during the transfer (see eq 1).

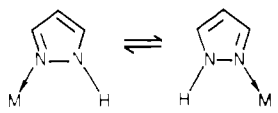

(1)

Several studies of pyrazole complexes of platinum and palladium have been published recently, especially $[M(pz)_2(L\text{-}L)]$ and $[M(pzH)_2(L\text{-}L)]^{2+}$, where M = Pt or Pd, pzH = pyrazole or substituted pyrazole, and L-L = 1,2-bis(diphenylphosphino)ethane, 2,2′-bipyridine, or cycloocta-1,5-diene.[8-10] However, no fluxional behavior has been reported in any of these studies. Fluxional behavior in the rhodium complex $[RhCl(pzH)CO)_2]$ has been noted in a preliminary communication, but no details have been published.[11] In the present paper we describe the synthesis of a series of cationic pyrazole and substituted-pyrazole complexes of platinum and palladium. The monodentate nature of the pyrazole ligands is demonstrated by an X-ray structure determination for the

(1) Eaton, S. S.; Eaton, G. R.; Holm, R. H. *J. Organomet. Chem.* **1972**, *39*, 179.
(2) (a) Cotton, F. A.; Ciapennelli, D. J. *Synth. Inorg. Met.-Org. Chem.* **1972**, *2*, 197. (b) Torocheshnikou, V. N.; Sergeyev, N. M.; Viktorov, N. A.; Goldin, G. S.; Poddubny, V. G.; Koltsoua, A. N. *J. Organomet. Chem.* **1974**, *70*, 347. (c) Cotton, F. A. In "Dynamic Nuclear Magnetic Resonance Spectroscopy"; Jackman, L. M., Cotton, F. A., Eds.; Academic Press: New York, 1975; Chapter 10.
(3) Bonny, A.; Stobart, S. R. *J. Am. Chem. Soc.* **1979**, *101*, 2247. Holmes-Smith, R. D.; Stobart, S. R. *Ibid.* **1980**, *102*, 382.
(4) Dixon, K. R. *Inorg. Chem.* **1977**, *16*, 2618 and references therein.
(5) Bushnell, G. W.; Dixon, K. R.; Khan, M. A. *Can. J. Chem.* **1978**, *56*, 450.
(6) Bushnell, G. W.; Dixon, K. R. *Can. J. Chem.* **1978**, *56*, 878.
(7) Brandon, J. B.; Collins, M.; Dixon, K. R. *Can. J. Chem.* **1978**, *56*, 950.
(8) Bonati, F.; Clark, H. C. *Can. J. Chem.* **1978**, *56*, 2513.
(9) Minghetti, G.; Banditelli, G.; Bonati, F. *J. Chem. Soc., Dalton Trans.* **1979**, 1851.
(10) Bandini, A. L.; Banditelli, G.; Minghetti, G.; Bonati, F. *Can. J. Chem.* **1979**, *57*, 3237.
(11) Borkett, N. F.; Bruce, M. I. *J. Organomet. Chem.* **1974**, *65*, C51.

0020-1669/81/1320-1545$01.25/0

Table I. Crystal Data for *cis*-[Pd(PEt_3)$_2$Cl(3,5-DMP)]

cryst system	triclinic	vol, Å^3	1305 (2)
space group	$P\bar{1}$	formula	$C_{17}H_{38}BClF_4N_2P_2Pd$
a, Å	11.45 (1)		
b, Å	15.483 (7)	fw	561.10
c, Å	9.92 (1)	Z	2
α, deg	90.8 (1)	d(measd), g cm^{-3}	1.44
β, deg	131.62 (5)	d(calcd), g cm^{-3}	1.43
γ, deg	94.6 (1)	μ(Mo K$\bar{\alpha}$), cm^{-1}	9.58

complex *cis*-[PdCl(3,5-dimethylpyrazole)(PEt_3)$_2$][BF_4], and we find that at ambient temperatures all of the palladium complexes studied exhibit a rapid metal/proton-transfer process.

Results

Synthesis and Characterization. The complexes were all prepared by cleavage reactions of chloro-bridged compounds according to eq 2, where M = Pt or Pd, Y = BF_4 or ClO_4,

$$[M_2Cl_2(PEt_3)_4][Y]_2 + 2L \rightarrow \textit{cis}\text{-}[MCl(PEt_3)_2L][Y] \quad (2)$$

and L = pyrazole (pzH), 3,5-dimethylpyrazole (3,5-DMP), 3,4,5-trimethylpyrazole (3,4,5-TMP), or 4-bromo-3,5-dimethylpyrazole (Br-3,5-DMP), which is a generally useful route to complexes having exclusively cis stereochemistry.[12] The products are all air-stable, colorless, crystalline solids which, except for the unsubstituted-pyrazole derivatives, dissolve readily in polar organic solvents but are insoluble in nonpolar solvents.

Preliminary characterization of the complexes was by C, H, and N microanalysis[13] and by infrared spectra, which showed all the expected ligand and anion absorptions together with ν(M–Cl) absorptions at ca. 300 cm^{-1}. The ν(M–Cl) absorptions were very weak in the palladium complexes. In both platinum and palladium complexes ν(N–H) occurred as a broad (width at half-height ~100 cm^{-1}) band at ca. 3200 cm^{-1}. Further characterization of the palladium complexes was achieved by observation of the parent cation using chemical ionization mass spectroscopy. However, the full characterization of the complexes rests primarily on the X-ray and variable-temperature NMR results described below.

Crystal and Molecular Structure of *cis*-[PdCl(PEt_3)$_2$(3,5-DMP)][BF_4]. The molecular structure of this complex is shown in Figure 1, and the crystal packing arrangement in Figure 2. Crystal data and atomic coordinates are given in Tables I and II, respectively. The structural results bear a close relationship to our previous studies of the series of complex cations *cis*-[PtCl(PEt_3)$_2$L]$^+$, where L = phenanthroline,[14] naphthyridine,[5] or phthalazine,[6] and frequent comparisons with this data will be made in the following presentation.

If the well-known trans influence for Pt complexes[15] is taken into account, the bond lengths given in Table III are normal and comparison with the results for the platinum series shows that the difference in size between Pd and Pt is small. Within the five-membered ring of the 3,5-DMP ligand the bond lengths and angles are very closely similar to those derived for the gaseous pyrazole molecule by accurate spectroscopic methods.[16] The hydrogen atoms of the heterocyclic ligand were located by the use of difference maps. Although true C–H bond lengths are known to be 1.07–1.09 Å, X-ray diffraction studies commonly give C–H lengths of about 0.97 Å. A similar discrepancy is found for N–H bond lengths, which are a few picometers shorter. From these criteria, the positions of the hydrogen atoms found are evidently inaccurate, but it was the proof of the presence of H(2) on N(2) that was important in this study.

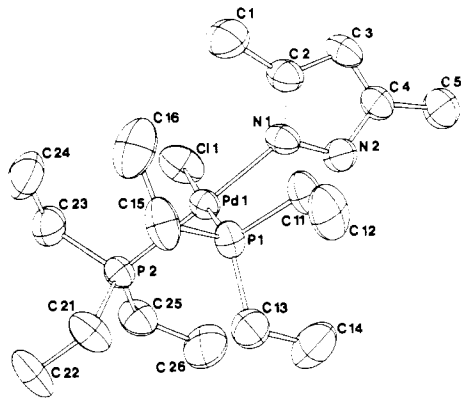

Figure 1. Molecular structure of *cis*-[PdCl(PEt_3)$_2$(3,5-DMP)][BF_4].

The bond angles are given in Table IV. The angles at Pd are very similar to those of the series of platinum complexes.[5,6,14] The angle P–Pd–P is considerably greater than 90° owing to steric effects. The angles at P are normal, with the Pd–P–C and C–P–C angles tending to be respectively greater and less than the tetrahedral value. The P–C–C angles are all close to the mean value of 114.5°. There is a considerable difference between the angles Pd–N(1)–C(2) and Pd–N(1)–N(2), external to the pyrazole ring, probably caused by (i) the steric effect of the *C(1)*-methyl group being greater than that of the hydrogen atom on N(2) and (ii) hydrogen bonding to be discussed later. The further set of four external angles show that the *C(1)*- and *C(5)*-methyl groups are significantly bent away from C(3) and toward the nitrogen atoms.

The results of the mean plane calculations are presented in Table V. The heterocyclic ligand is at right angles to the coordination plane. The five-membered ring defines plane 1, which passes close to the methyl carbon atoms C(1) and C(5). The Pd atom is –0.3482 Å from plane 1, and the cause of this is probably steric repulsion between the first PEt_3 group and the 3,5-dimethylpyrazole ring. The atoms Pd, Cl, P(2), C(1), and C(5) all lie on the same side of plane 1. The definition of the coordination plane is not straightforward because the Pd atom and the four atoms bonded to it form a nonplanar set. The exact plane through Pd, P(1), and P(2) (plane 2) is therefore used as the reference plane. Two ethyl groups, one from each phosphine ligand, lie very close to plane 2. Cl and N(1) lie off plane 2 by +0.118 (3) and –0.078 (7) Å, respectively. Cl and C(1) are on the opposite side of the reference plane from N(1) and N(2).

The conformations of the triethylphosphine ligands are similar to those in related complexes[5,6,14] and cannot provide an explanation for the slight nonplanarity of the Pd coordination.

The interionic contacts are all >3.47 Å except for that between F(2) and N(2), which is 2.79 (1) Å, indicating that there is a hydrogen bond F(2)···H(2)–N(2) linking the cation to the anion. This provides confirmation that a hydrogen atom is bound to N(2) in the structure. The value of 161° for angle F(2)···H(2)–N(2) is reasonable. The hydrogen bond explains the nonplanarity of the Pd coordination and why both N atoms are on the same side of the PPdP plane (see Figure 2). The reason the Cl atom is out of the coordination plane may be the Cl–C(16) contact (3.548 (9) Å), the nature of which can easily be seen by concentrating on the molecule closest to the origin in Figure 2, taking the labels from Figure 1, and noting

(12) Dixon, K. R.; Moss, K. C.; Smith, M. A. R. *Can. J. Chem.* **1974**, *52*, 692.
(13) Microanalytical figures were supplied for perusal by the referees and are included in the supplementary tables.
(14) Bushnell, G. W.; Dixon, K. R.; Khan, M. A. *Can. J. Chem.* **1974**, *52*, 1367.
(15) Hartley, F. R. *Chem. Soc. Rev.* **1973**, *2*, 163.
(16) Harmony, M. D.; et al. *J. Phys. Chem. Ref. Data* **1979**, *8*, 693.

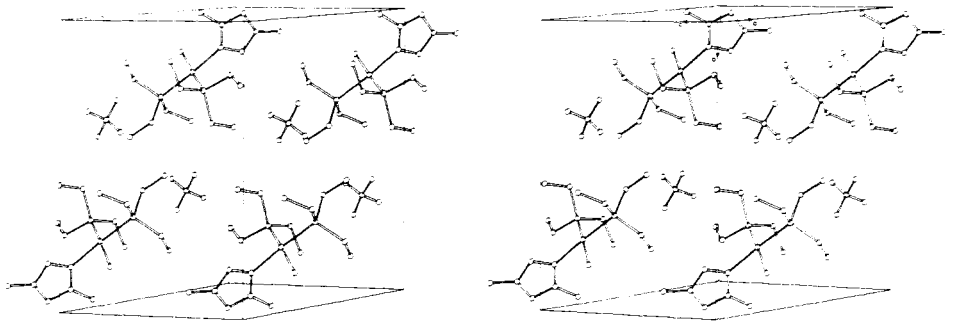

Figure 2. Stereoscopic view of the crystal packing of *cis*-$[PdCl(PEt_3)_2(3,5\text{-DMP})][BF_4]$.

Table II. Fractional Atomic Coordinates ($\times 10^4$) and Thermal Parameters ($\times 10^3$) for *cis*-$[Pd(PEt_3)_2Cl(3,5\text{-DMP})]$ ($Å^2$)[a]

atom	x	y	z	U_{11}	U_{22}	U_{33}	U_{12}	U_{13}	U_{23}
Pd	−2339.5 (5)	2218.1 (3)	−44.7 (6)	34.9 (3)	41.1 (2)	44.5 (3)	4.8 (2)	26.0 (2)	−0.3 (2)
Cl	−246 (2)	1608 (1)	2566 (3)	55 (1)	71 (1)	56 (1)	32 (1)	21 (1)	9 (1)
P(1)	−4445 (2)	2712 (1)	−2659 (2)	46 (1)	58 (1)	41 (1)	15.2 (7)	30 (1)	7 (1)
P(2)	−2176 (2)	3123 (1)	1935 (2)	38 (1)	46 (1)	39.2 (8)	5.3 (7)	24 (1)	−1.2 (6)
F(1)	2566 (10)	2893 (6)	−673 (13)	181 (8)	182 (8)	210 (9)	52 (7)	148 (8)	−10 (7)
F(2)	612 (9)	3145 (4)	−911 (12)	142 (6)	96 (5)	268 (10)	−8 (4)	161 (7)	6 (5)
F(3)	2565 (9)	4133 (5)	384 (10)	154 (6)	120 (5)	143 (6)	−23 (5)	79 (5)	−39 (4)
F(4)	1000 (15)	3823 (7)	−2459 (11)	367 (14)	237 (10)	106 (5)	−2 (9)	144 (8)	44 (6)
N(1)	−2100 (6)	1337 (3)	−1456 (7)	40 (3)	42 (4)	60 (4)	5 (3)	32 (3)	−4 (3)
N(2)	−1111 (6)	1532 (4)	−1745 (8)	54 (4)	50 (4)	77 (4)	11 (3)	50 (3)	9 (3)
C(1)	−3657 (10)	44 (5)	−1754 (13)	81 (6)	72 (6)	115 (7)	−9 (5)	72 (6)	−8 (5)
C(2)	−2559 (8)	495 (4)	−1926 (9)	52 (4)	49 (4)	63 (4)	−1 (3)	38 (4)	−8 (4)
C(3)	−1858 (9)	153 (4)	−2510 (10)	76 (5)	48 (5)	73 (5)	15 (4)	53 (5)	−3 (4)
C(4)	−935 (8)	819 (4)	−2367 (10)	66 (5)	53 (5)	73 (5)	21 (4)	53 (4)	9 (4)
C(5)	113 (11)	863 (5)	−2781 (13)	113 (7)	75 (6)	129 (8)	33 (5)	103 (7)	18 (5)
C(11)	−4945 (8)	2130 (5)	−4641 (9)	62 (4)	78 (5)	41 (4)	17 (4)	34 (4)	2 (4)
C(12)	−6337 (10)	2408 (6)	−6471 (10)	90 (6)	120 (7)	43 (4)	32 (5)	39 (5)	13 (5)
C(13)	−4259 (10)	3858 (5)	−2980 (10)	101 (6)	66 (5)	71 (5)	28 (5)	63 (5)	23 (4)
C(14)	−2981 (13)	4093 (6)	−2996 (14)	139 (9)	93 (7)	128 (9)	−3 (7)	104 (8)	21 (6)
C(15)	−6286 (8)	2529 (6)	−3093 (9)	40 (4)	111 (6)	50 (4)	19 (4)	28 (4)	0 (4)
C(16)	−6658 (9)	1623 (7)	−2887 (12)	48 (5)	147 (10)	77 (6)	−9 (5)	39 (5)	12 (6)
C(21)	−3562 (9)	3923 (5)	1116 (10)	68 (5)	74 (5)	62 (5)	25 (4)	37 (5)	−4 (4)
C(22)	−3303 (10)	4478 (6)	2614 (11)	97 (7)	101 (7)	78 (6)	42 (5)	59 (5)	−10 (5)
C(23)	−2240 (9)	2498 (5)	3453 (10)	78 (6)	74 (5)	59 (5)	2 (4)	49 (5)	1 (4)
C(24)	−3645 (11)	1839 (6)	2543 (13)	108 (8)	108 (7)	105 (8)	−23 (6)	85 (7)	−3 (6)
C(25)	−237 (8)	3748 (5)	3448 (10)	48 (4)	66 (5)	65 (5)	−10 (3)	33 (4)	−20 (4)
C(26)	276 (11)	4127 (6)	2504 (14)	104 (8)	92 (7)	118 (8)	−42 (6)	82 (7)	−26 (6)
B	1656 (15)	3500 (8)	−960 (16)	97 (9)	73 (7)	74 (7)	1 (7)	63 (7)	−1 (6)

[a] $T = \exp[-2\pi^2(U_{11}h^2a^{*2} + \ldots + 2U_{12}hka^*b^* + \ldots)]$.

Table III. Bond Lengths ($\times 10^2$; Å)

Pd-Cl	235.2 (4)	B-F(1)	135 (1)
Pd-P(1)	227.4 (4)	B-F(2)	131 (1)
Pd-P(2)	229.0 (4)	B-F(3)	133 (1)
Pd-N(1)	210.2 (2)	B-F(4)	127 (1)
P(1)-C(11)	183.9 (7)	P(2)-C(21)	182.9 (8)
P(1)-C(13)	182.8 (8)	P(2)-C(23)	184.0 (8)
P(1)-C(15)	184.5 (7)	P(2)-C(25)	181.8 (7)
C(11)-C(12)	152 (1)	C(21)-C(22)	154 (1)
C(13)-C(14)	149 (1)	C(23)-C(24)	149 (1)
C(15)-C(16)	149 (1)	C(25)-C(26)	150 (1)
C(1)-C(2)	150 (1)	C(4)-C(5)	150 (1)
C(2)-C(3)	139.3 (9)	C(3)-C(4)	135 (1)
N(1)-C(2)	131.9 (7)	N(2)-C(4)	134.9 (6)
N(1)-N(2)	135.5 (9)	Pd-H(2)	320
C(1)-H(11)	107	C(5)-H(51)	102
C(1)-H(12)	110	C(5)-H(52)	109
C(1)-H(13)	103	C(5)-H(53)	106
N(2)-H(2)	88	C(3)-H(3)	103

Table IV. Bond Angles (Deg)

N(1)-Pd-P(1)	91.9 (1)	N(1)-Pd-Cl	85.5 (1)
P(1)-Pd-P(2)	97.9 (1)	P(1)-Pd-Cl	176.02 (7)
P(2)-Pd-Cl	84.9 (1)	P(2)-Pd-N(1)	169.95 (5)
Pd-P(1)-C(11)	111.1 (2)	Pd-P(2)-C(21)	121.0 (3)
Pd-P(1)-C(13)	117.6 (3)	Pd-P(2)-C(23)	111.1 (3)
Pd-P(1)-C(15)	114.3 (3)	Pd-P(2)-C(25)	108.4 (3)
C(11)-P(1)-C(13)	103.8 (4)	C(21)-P(2)-C(23)	105.7 (4)
C(13)-P(1)-C(15)	105.2 (4)	C(23)-P(2)-C(25)	104.0 (4)
C(15)-P(1)-C(11)	103.4 (4)	C(25)-P(2)-C(21)	105.3 (4)
P(1)-C(11)-C(12)	115.8 (5)	P(2)-C(21)-C(22)	114.7 (5)
P(1)-C(13)-C(14)	113.0 (6)	P(2)-C(23)-C(24)	115.7 (6)
P(1)-C(15)-C(16)	114.0 (6)	P(2)-C(25)-C(26)	114.0 (6)
Pd-N(1)-C(2)	131.0 (3)	Pd-N(1)-N(2)	122.4 (1)
C(1)-C(2)-C(3)	129.5 (6)	C(1)-C(2)-N(1)	120.4 (6)
C(5)-C(4)-C(3)	132.0 (7)	C(5)-C(4)-N(2)	121.7 (6)
N(1)-C(2)-C(3)	110.1 (6)	C(4)-N(2)-N(1)	111.4 (6)
C(2)-C(3)-C(4)	106.7 (6)	N(2)-N(1)-C(2)	105.5 (6)
C(3)-C(4)-N(2)	106.3 (6)	F(2)-H(2)-N(2)	161
H(2)-N(2)-N(1)	125	H(2)-N(2)-C(4)	123
H(3)-C(3)-C(2)	113	H(3)-C(3)-C(4)	139
F(1)-B-F(2)	108 (1)	F(2)-B-F(3)	108 (1)
F(1)-B-F(3)	108 (1)	F(3)-B-F(4)	109 (1)
F(1)-B-F(4)	111 (1)	F(4)-B-F(2)	111 (1)

that the symmetry position involved is found by translation along the vector $a + c$. A shortage of space around Pd in the coordination plane might also contribute to an out-of-plane Cl displacement on the opposite side from N(1).

Variable-Temperature NMR. (a) *cis*-$[PdCl(PEt_3)_2(Br\text{-}3,5\text{-DMP})][ClO_4]$. Our most complete set of variable-temperature data was obtained for this complex. The limiting low-temperature (<233 K) ^1H spectrum in dichloromethane solution showed separate singlet resonances for the 3- and 5-methyl groups (δ 2.33 and 2.30), a multiplet attributable

Table V. Planes through Selected Sets of Atoms

atom	P,[a] Å	atom	P,[a] Å
Plane 1: N(1), N(2), C(2), C(3), C(4);[b,c] $\chi^2 = 1.74$[d]			
$-0.2165X + 0.2738Y - 0.9371Z = 1.9503$ (Å)[e]			
N(1)	−0.002 (5)	Pd	−0.3482 (5)
N(2)	0.004 (6)	C(1)	−0.03 (1)
C(2)	0.000 (7)	C(5)	−0.01 (1)
C(3)	0.004 (8)	H(2)	0.15
C(4)	−0.007 (7)	H(3)	−0.17
Plane 2: Pd, P(1), P(2)[b]			
$-0.7389X - 0.6727Y - 0.0398Z = -0.1423$ (Å)			
Cl	0.118 (3)	N(1)	−0.078 (7)
C(11)	−0.02 (1)	C(21)	0.00 (1)
C(12)	−0.03 (1)	C(22)	0.01 (1)

[a] P is the perpendicular distance of an atom from the plane. [b] The dihedral angle between planes 1 and 2 is 89.3°. [c] Plane 1 is a least-squares plane. [d] $\chi^2 = \Sigma_i(P_i^2/\sigma^2(P_i))$, where i ranges over all atoms defining the plane. [e] X, Y, Z are coordinates in Å with respect to an orthogonal axis system with X along a, Y in the ab plane, and Z along c^*.

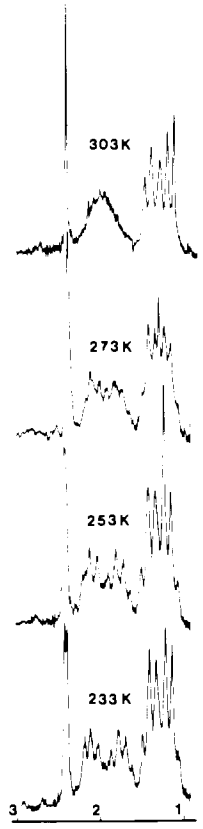

Figure 3. ^{1}H NMR spectra of *cis*-[PdCl(PEt$_3$)$_2$(Br-3,5-DMP)][ClO$_4$] recorded at 90 MHz in dichloromethane solution in the temperature range 233–303 K. Chemical shift scale is ppm downfield of Me$_4$Si.

to the methyl groups of the phosphine ligands centered at δ 1.2, and two separate multiplets assigned to the methylene groups of two nonequivalent phosphine ligands centered at δ 2.0 and 1.7. This spectrum is shown in Figure 3 together with spectra at other temperatures. Figure 4 shows proton-decoupled ^{31}P spectra obtained for the same complex in 1,2-dichloroethane solution[17] together with corresponding simulated spectra.[18] The limiting low-temperature spectrum in this case is an AB quartet assignable to two nonequivalent phosphorus atoms (δ −105.4 and −109.9) in a mutally cis configuration as shown by the low value of ^2J(P–P), namely, 14.5 Hz. A trans configuration would be expected to give a single ^{31}P resonance.

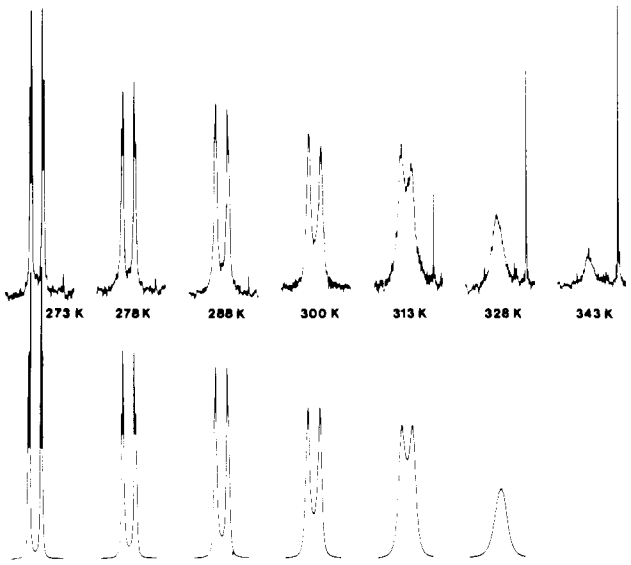

Figure 4. ^{31}P{^{1}H} NMR spectra of *cis*-[PdCl(PEt$_3$)$_2$(Br-3,5-DMP)][ClO$_4$] recorded at 24.3 MHz in 1,2-dichloroethane solution in the temperature range 273–343 K. The upper traces at each temperature are observed spectra and the lower traces are simulated by the DNMR3 computer program.

Table VI. Rate Constants k (s^{-1}) for Fluxional Processes in [PdCl(PEt$_3$)$_2$(Br-3,5-DMP)] [ClO$_4$]

	phosphorus interchange				3,5-dimethyl interchange
	a		*b*	*c*	^{1}H data in CH$_2$Cl$_2$
temp, K	δ_{AB}, Hz	k	k	k	k
233			<5		4
243				5	
253					8
273	108	10	25	26	12
278	110	23			
288	114	42		38	
300	119	90	70	95	50
313	134	200			
328	160	450			

[a] Data from ^{31}P spectra in 1,2-dichloroethane. [b] Data from ^{1}H spectra (CH$_2$ resonances in PEt$_3$ groups) in dichloromethane. [c] Data from ^{31}P spectra in dichloromethane.

Thus, the low-temperature spectra are fully consistent with a static solution structure similar to that found in the crystalline state for *cis*-[PdCl(PEt$_3$)$_2$(3,5-DMP)][BF$_4$]. Raising the temperature produces the spectral changes shown in Figures 3 and 4, and comparison of the observed and calculated line shapes gives rate data from three different processes: first the coalescence of the AB quartet in the ^{31}P spectrum, second the coalescence of the 3- and 5-methyl resonances in the ^{1}H spectrum, and finally the collapse of the two nonequivalent phosphine ligand methylene resonances in the ^{1}H spectrum. Rate constants from all three sources are collected in Table VI, and some of these data are plotted in Figure 5.

(i) ^{31}P Resonances. A complete set of variable-temperature ^{31}P spectra obtained in 1,2-dichloroethane solution is shown in Figure 4. Preliminary simulations made it clear that the

(17) Spectra in dichloromethane were similar, but the boiling point of this solvent is too low to permit a full range of variable-temperature spectra. Solubility in 1,2-dichloroethane was too low to permit ready determination of low-temperature ^{1}H spectra on our continuous-wave instrument—hence the use of two different solvents.

(18) All simulated spectra were computed by using the DNMR3 program: Kleier, D. A.; Binsch, D. Program 165, Quantum Chemistry Program Exchange, Indiana University, 1969.

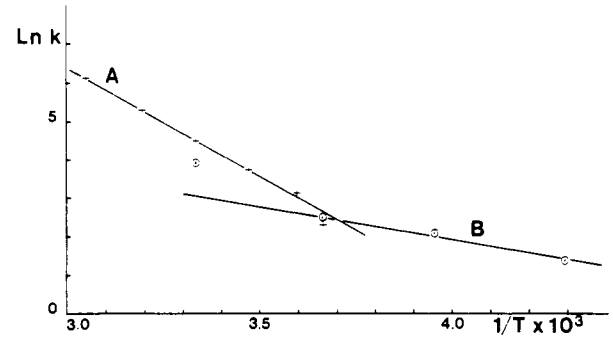

Figure 5. Arrhenius plots (ln k against $1/T$) derived from computer simulation of NMR spectra of *cis*-$[PdCl(PEt_3)_2(Br\text{-}3,5\text{-}DMP)][ClO_4]$. Plot A (crosses) is for $^{31}P\{^1H\}$ spectra recorded in 1,2-dichloroethane solution and plot B (circles) is for 3,5-dimethyl interchange as recorded by ^1H spectra in dichloromethane solution (i.e., the last column of Table VI).

observed line shapes at 300, 313, and 328 K can only be satisfactorily fitted if δ_{AB} is assumed to increase with temperature. The correct choice of δ_{AB} remains well defined until near the coalescence point, but at higher temperatures the choices of rate constant (k) and δ_{AB} are critically interrelated. The other important parameter is the choise of transverse relaxation time ($T_2 = 1/\pi W$, where W = width at half-height of peaks not broadened by exchange). This parameter choice (5-Hz line width in Figure 2) has a critical effect in the low-temperature region, where resolution of J_{AB} is collapsing but the A and B regions are still resolved. Once A and B begin to coalesce, the choice of line width is not critical. With the uncertainties in δ_{AB} and in T_2, estimation of the reliability of the absolute rate data given in Table VI must be approached with caution.

The data are, however, reliable in indicating approximate relative rates and the qualitative nature of the exchange processes. Thus, it is clear that in the temperature range 273–313 K the principal exchange process is one which renders the two phosphorus sites equivalent. These spectra are "fully reversible" on recooling the sample. Above about 313 K the spectra (see Figure 4) begin to exhibit a new, sharp single resonance at δ −118.4. We assign this resonance to *trans*-$[PdCl(PEt_3)_2(Br\text{-}3,5\text{-}DMP)]^+$, and formation of this isomer does not reverse on lowering the temperature. Unfortunately, however, it does reverse on crystallization of the sample, and consequently we were not able to confirm this assignment by full characterization of a crystalline sample. Attempts to prepare the trans isomer by reactions of *trans*-$[PdCl_2(PEt_3)_2]$ with Br-3,5-DMP and $NaClO_4$ or $AgBF_4$ also failed. However, it is known that tertiary phosphine resonances in trans palladium complexes are generally sharper and are to high field of the corresponding cis complexes.[19] These points, together with the simplicity of the system and the spectra, strongly suggest that the assignment is correct.

For comparison of rates with the low-temperature ^1H spectra recorded in dichloromethane (see below) a partial set of variable-temperature ^{31}P spectra was recorded in this solvent. Rates are shown in Table VI, but the low boiling point of dichloromethane precluded determination of a full data set.

(ii) 3,5-Methyl Resonances. Again the principal problem is to derive values for the true chemical shift difference ($\delta_{3,5}$ in this case) and for the line width. Fortunately, the 233 K (Figure 3) and 213 K (not illustrated) spectra were very similar. Thus the low-temperature limit has been reached, and values of δ_{AB} = 4 Hz and line width = 1.6 Hz may be derived from the observed line shape. Simulation of the spectra at various temperatures yields the rate data collected in Table VI and used in plotting Figure 5. As with the ^{31}P data, the precise values of the rates are critically dependent on the choice of line width. However, the results clearly demonstrate that as averaging occurs between the nonequivalent phosphorus positions, the 3- and 5-methyl positions on the pyrazole ligand are also rendered equivalent. Comparison of the rate of methyl site averaging with that of the phosphorus process is complicated by the necessity to use two different solvents to cover the temperature ranges involved. This necessity arises because the coalescence temperature for the 3,5-methyl ^1H resonance is ~250 K whereas for the ^{31}P resonances it is ~320 K. Figure 5 and Table VI show that site averagings for the methyl groups in dichloromethane and for the phosphorus nuclei in 1,2-dichloroethane are, at 273 K, approximately equal in rate.

(iii) Methylene Resonances. The rates of coalescence of these two broad multiplets were estimated by using DNMR3[18] to treat the system as very broad singlets. This gives some very approximate data, which are included in Table VIII as a confirmation of the ^{31}P data and as a cross reference between the two solvents and sets of ^1H and ^{31}P spectra.

(b) Other *cis*-$[PdCl(PEt_3)_2L][Y]$ Complexes. Spectra of the complexes where L = 3,5-DMP or 3,4,5-TMP were studied on BF_4^- salts. Results were essentially identical with those described above for L = Br-3,5-DMP and showed the same temperature change over similar temperature ranges. For L = 3,5-DMP, the low-temperature limiting ^{31}P spectrum (273 K in CH_2Cl_2) gave δ −106.2 and −108.8 and $^2J(P\text{–}P)$ = 14.8 Hz; and the low-temperature limiting ^1H spectrum (213 K in $CDCl_3$) gave δ 6.0 (4-H), δ 2.40, 2.37 (3,5-CH_3), δ 2.1, 1.7 (CH_2 in PEt_3), and δ 1.25 (CH_3 in PEt_3). For L = 3,4,5-TMP, the low-temperature limiting ^{31}P spectrum (273 K in CH_2Cl_2) gave δ −106.6 and −108.6 and $^2J(P\text{–}P)$ = 15.4 Hz; and the low-temperature limiting ^1H spectrum (233 K in CH_2Cl_2) gave δ 2.25, 2.20 (3,5-CH_3), δ 1.83 (4-CH_3), δ 2.0, 1.6 (CH_2 in PEt_3), and δ 1.15 (CH_3 in PEt_3).

The complex for L = pyrazole and Y = ClO_4 was too insoluble for effective NMR study and was characterized only by microanalysis and infrared spectroscopy.

(c) *cis*-$[PtCl(PEt_3)_2(3,5\text{-}DMP)]ClO_4$. At ambient temperature (300 K) in dichloromethane solution, the ^{31}P spectrum of this complex consisted of an AB quartet (close to AX) with sidebands due to coupling with ^{195}Pt (33.8% abundant, I = $^1/_2$): δ_A −131.0, δ_B −135.2, $^1J(Pt\text{–}P_A)$ = 3460 Hz, $^1J(Pt\text{–}P_B)$ = 3166 Hz, $^2J(P_A\text{–}P_B)$ = 20.4 Hz. These data clearly support a cis stereochemistry and indicate that the complex is nonfluxional. Most trans influence series based on NMR coupling constants in platinum complexes place nitrogen > chlorine.[20] Hence on the basis of $^1J(Pt\text{–}P_B)$ being less than $^1J(Pt\text{–}P_A)$ we may assign the P_A resonance to phosphorus trans to chlorine and the P_B resonance to phosphorus trans to nitrogen. Proton spectra were also nonfluxional with, for example, spectra at 293 K in $CDCl_3$ giving δ 6.0 (4-H), δ 2.43, 2.37 (3,5-CH_3), δ 2.1, 1.8 (CH_2 in PEt_3), and δ 1.2 (CH_3 in PEt_3) and showing no significant changes up to the boiling point of the solvent (~330 K). Attempts to obtain higher temperature spectra in dimethyl sulfoxide solution were not useful because the 3,5 resonances were not resolved in this solvent.

The temperature dependence of the ^{31}P spectrum was studied from 213 to 373 K with dichloromethane as solvent below ambient temperature and dimethyl sulfoxide above ambient temperature. Throughout this temperature range the spectra exhibited no changes attributable to fluxional processes, and above 373 K the sample began to decompose. However, there were some very marked and interesting changes due

(19) Redfield, D. A.; Cary, L. W.; Nelson, J. H. *Inorg. Chem.* **1975**, *14*, 50. Verstuyft, A. W.; Redfield, D. A.; Cary, L. W.; Nelson, J. H. *Ibid.* **1977**, *16*, 2776.

(20) Appleton, T. G.; Clark, H. C.; Manzer, L. E. *Coord. Chem. Rev.* **1973**, *10*, 335.

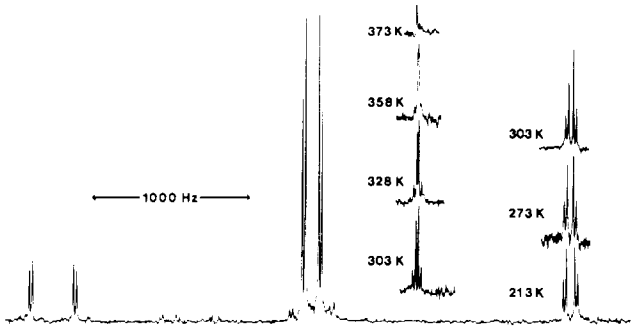

Figure 6. $^{31}P\{^1H\}$ NMR spectra of *cis*-$[PtCl(PEt_3)_2(3,5\text{-}DMP)][ClO_4]$ recorded at 24.3 MHz. The low-field sideband and the center band remain unchanged as temperature varies (except for small positional shifts) while the upfield sideband shows the illustrated changes. The low-temperature spectra (right-hand set) are in dichloromethane solution and the high-temperature spectra (left-hand set) in dimethyl sulfoxide

primarily to a differential temperature dependence between the two platinum–phosphorus coupling constants. As we have pointed out previously,[21] ^{195}Pt sideband spectra are not necessarily identical with the center band spectra. In particular, when the center band is a closely coupled system such as A_nB_m, the sideband spectra will belong to an A_nB_mM spin system and will be analyzable as two A_nB_m subspectra with effective chemical shifts $\delta_{AB} \pm {}^1/_2(J_{AM} - J_{BM})$.[21] In the present example, the low-field sideband and the center band remain as weakly coupled AB systems throughout the temperature range studied while changes in J_{AM} and J_{BM} (M = ^{195}Pt) cause the upfield sideband to change from a weakly coupled AB at 213 K to a very closely coupled system at 373 K. The effect is shown in Figure 6 and could be easily mistaken for a fluxional process. The changes are caused by the temperature dependence of $^1J(Pt\text{–}P_B)$, the coupling constant trans to the pyrazole ligand, which changes in dichloromethane from 3121 Hz at 213 K to 3167 Hz at 300 K and then in dimethyl sulfoxide from 3123 Hz at 300 K to 3163 Hz at 373 K. The trend in both solvents is approximately linear with temperature, and the slope of a plot of J vs. temperature is the same in both solvents. The chemical shifts of P_A and P_B also change approximately linearly with temperature (~0.01 ppm deg^{-1}), but the separation of δ_A and δ_B (5.76 ppm in dimethyl sulfoxide, 4.20 ppm in dichloromethane) is almost independent of temperature. The coupling constant trans to chlorine, $^1J(Pt\text{–}P_A)$, is also almost independent of temperature, decreasing by only ~10 Hz from 213 to 373 K.

The increase with temperature of $^1J(Pt\text{–}P_B)$ in *cis*-$[PtCl(PEt_3)_2(3,5\text{-}DMP]ClO_4$ is an effect similar to that observed previously[22] in our detailed study of solvent, concentration, and temperature dependence of $^1J(Pt\text{–}P)$ in *cis*- and *trans*-$[PtCl_2(P\text{-}n\text{-}Bu_3)_2]$. As in that case the present results show temperature variation in the reverse direction to those observed previously for $^1J(P\text{–}H)$ in phosphine.[23] A model involving temperature decrease of specific axial solvation of the platinum complex with corresponding increase in the availability of the Pt 6s orbital for Pt–P bonding was proposed by us for the *cis*- and *trans*-$[PtCl_2(P\text{-}n\text{-}Bu_3)_2]$ cases[22] and may also be invoked to explain the *cis*-$[PtCl(PEt_3)_2(3,5\text{-}DMP)]ClO_4$ results. In the latter case it is not clear why only the Pt–P bond trans to nitrogen is significantly affected.

(d) Other *cis*-$[PtCl(PEt_3)_2L]Y$ Complexes. The complexes where L = 3,4,5-TMP or pzH were studied as ClO_4^- salts. Spectra of the former complex were essentially identical with those described above for L = 3,5-DMP and yielded the following parameters. (a) ^{31}P spectrum in dichloromethane at 300 K: δ_A(trans to Cl) −131.7, δ_B(trans to N) −136.4, $^1J(Pt\text{–}P_A)$ = 3468 Hz, $^1J(Pt\text{–}P_B)$ = 3147 Hz, $^2J(P_a\text{–}P_B)$ = 20.4 Hz. (b) ^1H spectrum in deuteriochloroform at 300 K: δ 2.29 (3,5-CH_3), δ 1.90 (4-CH_3), δ 1.80, 2.08 (CH_2 in PEt_3), δ 1.18 (CH_3 in PEt_3). The latter complex was too insoluble for effective NMR study and was characterized only by microanalysis and infrared spectroscopy.

Discussion

The NMR data collected in the Results, principally for *cis*-$[PdCl(PEt_3)_2(Br\text{-}3,5\text{-}DMP)]ClO_4$, and in Figures 3–5 and Table VI clearly show that the behavior of the palladium complexes in solution can be described in terms of three distinct processes: (a) reversible averaging of the two phosphorus resonances

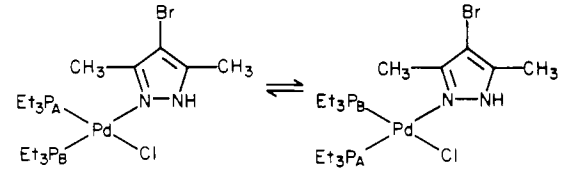

(b) reversible averaging of the 3- and 5-methyl resonances of the pyrazole ligand

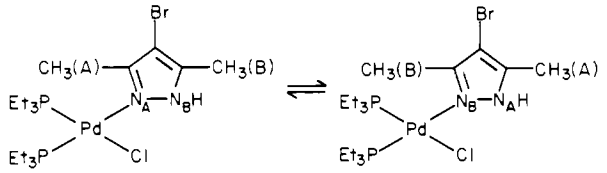

and (c) isomerization to a trans complex

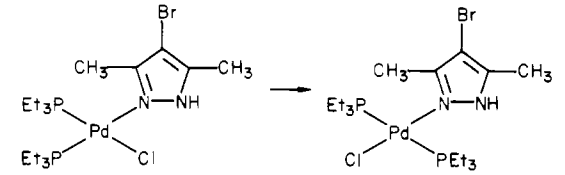

While processes a and b occur at comparable rates, reaction c is very much slower and only becomes significant at temperatures above ~310 K.

Figure 5 shows plots of ln K against $1/T$ for processes a (graph A) and b (graph B). Evaluation of the Arrhenius activation energies, E_a, from the slopes of these plots yields values of ~45 and ~15 kJ mol^{-1}, respectively, for the phosphorus site averaging and for the 3,5-methyl site averaging. Unfortunately, the widely differing coalescence temperatures for the two processes make it difficult to be sure whether graphs A and B are independent or are part of a single curve, but the essential observation of two differing Arrhenius activation energies is very clear.[24] At 273 K the two processes have closely similar rates (k ~ 10 s^{-1}), and use of the Eyring equation to obtain $\Delta G^{\ddagger}$ at this temperature gives ~60 kJ mol^{-1} for both processes. The Arrhenius activation energy (~45

(21) Dingle, T. W.; Dixon, K. R. *Inorg. Chem.* **1974**, *13*, 846.
(22) Dixon, K. R.; Fakley, M.; Pidcock, A. *Can. J. Chem.* **1976**, *54*, 2733.
(23) Ebsworth, E. A. V.; Sheldrick, G. M. *Trans. Faraday Soc.* **1967**, *63*, 1071.

(24) A reviewer has questioned whether uncertainties in the rate data could be sufficiently large to eliminate the two-slope pattern in Figure 5. However, changing both slopes to 30 kJ mol^{-1} would require minimum errors of ~100% in the rate constants, even if all errors were fortuitously in the correct directions. In fact, computer simulations varying δ_{AB} and T_2 indicate errors in the rate constants derived from ^{31}P spectra of ~5–10% near the coalescence point and possibly up to 25% at the temperature extremes. The ^1H data are less precise (up to perhaps 50% at the temperature extremes) but not sufficiently so to affect the conclusion.

Scheme I. Proposed Mechanism for Fluxional Rearrangement of Palladium Pyrazole Complexes

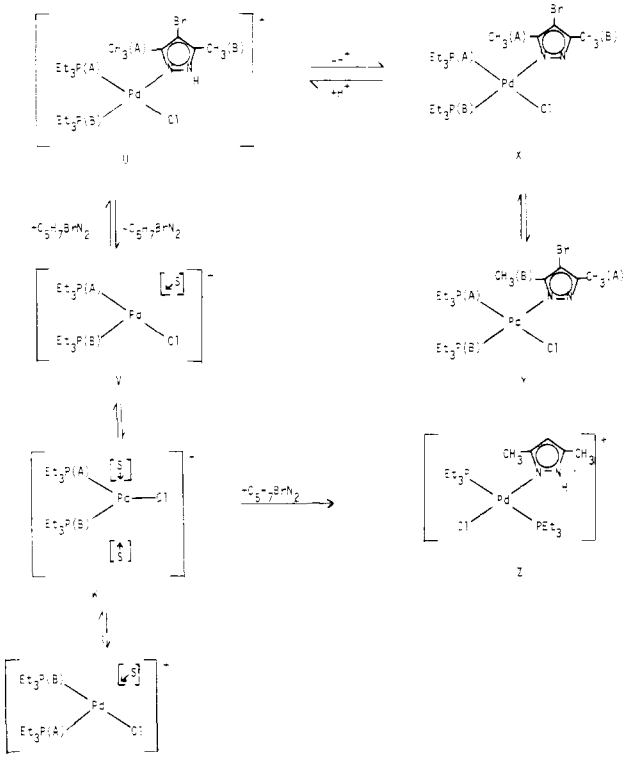

kJ mol^{-1}) for phosphorus site averaging is in good agreement with the ~50 kJ mol^{-1} obtained previously[7] for fluxional processes involving dissociation of the phthalazine ligand in *cis*-[PdCl(PEt$_3$)$_2$(phth)]$^+$. Thus in Scheme I we propose dissociation of the pyrazole ligand to form the intermediate V as the first and rate-controlling step in phosphorus site averaging in the palladium complexes. In the platinum analogues, generally being less labile and having stronger M–N bonds, this step is slower and the complexes are static on the NMR time scale. The "dissociation" step may be a result of ligand displacement by a solvent molecule and this possibility is taken into account in Scheme I. The phosphorus positions can then become equivalent, either through relaxation to a trigonal intermediate, W, or alternatively by a mechanism involving transient formation of the dinuclear cation [Pd$_2$(μ-Cl)$_2$(PEt$_3$)$_4$]$^{2+}$, possibly present in too low a concentration to be detectable by ^{31}P NMR.

Recoordination of the pyrazole ligand to W either re-forms the cis complex U or the trans isomer Z. Formation of the latter is evidently the slower reaction, but it leads to the formation of a stronger Pd–N bond, trans to Cl rather than PEt$_3$. Thus the back-reaction to W is slow, and the trans isomer accumulates as observed.

The other fragment from the dissociative reaction is a free pyrazole ligand. If proton transfer between the nitrogen atoms is relatively rapid (see below), this implies that the dissociative reaction will also lead to 3,5-methyl site averaging in the pyrazole and it appears that these processes dominate the kinetics in the high-temperature region (graph A). In our previous work with *cis*-[PdCl(PEt$_3$)$_2$(phth)]$^+$ phosphorus site averaging and averaging of the 2 and 7 protons of the phthalazine both had E_a ~ 50 kJ mol^{-1}, and consequently the dissociative mechanism appeared to be the only one operating.[7] However, in the pyrazole case the observation of a different E_a, ~15 kJ mol^{-1}, in the low-temperature region (graph B) suggests that a second mechanism may also be important. The nature of this second mechanism is more difficult to characterize, but we suggest that it proceeds via a deprotonated species, X. The rate of proton transfer between nitrogen atoms in uncoordinated pyrazole molecules has been a subject of recent debate in the literature. Most authors have found it to be a very rapid process on the NMR time scale at ambient temperature except in the most basic solvents (e.g., (Me$_2$N)$_3$PO),[25] but this conclusion has been questioned by a recent paper suggesting that previous observations of fast averaging in dimethyl sulfoxide were due to acidic impurities.[26] In the present case the acidity of the pyrazole proton is expected to be enhanced by inductive electron withdrawal caused by coordination to the metal and formation of X should be facile. The equilibrium between X and Y then leads to averaging of the 3- and 5-methyl positions of the pyrazole, but the exact nature of this process is not clear. The value of E_a of ~15 kJ mol^{-1} from graph B in Figure 5 is closely comparable with previously reported activation energies for proton transfer in pyrazoles[25,26] and could be associated with either the deprotonation to X or the X/Y equilibrium. In either case the low value, compared to ~50 kJ mol^{-1} for dissociative processes, suggests an intramolecular mechanism as a strong possibility. This could be analogous to the 1,2 (equivalent to 1,5) metallotropic shift described by Cotton and Ciappenelli[2a] for a 1-(trimethylgermyl)pyrazole derivative. In this context the nonfluxional character of the platinum pyrazole complexes is not surprising since it is known, for example, in iron and ruthenium cyclopentadienyl complexes,[2c] that rates of metallotropic shifts decrease down a transition metal triad.

If a dual mechanism process such as Scheme I is not adopted, the only way in which the two activation energies can be accommodated within a single dissociative mechanism is to assume that ligand dissociation is a fast initial step. In this case the larger value of E_a can be associated with formation of W from the initial cis solvent complex and the smaller value of E_a with proton transfer in the uncoordinated pyrazole. This possibility seems unlikely on the present evidence since it leads to an unrealistically low activation energy for an ambient-temperature bond dissociation process.

Another line of evidence which potentially bears on the question of intramolecular vs. dissociative mechanisms derives from the X-ray structural work. Our previous studies of fluxional processes in platinum[4] and palladium[7] complexes *cis*-[MCl(PEt$_3$)$_2$L]$^+$, where L was phenanthroline, naphthyridine, or phthalazine, showed that the rate of metal transfer between the two nitrogen sites decreased in the order phen > naph > phth. For platinum complexes of phenanthroline and naphthyridine where the nitrogen lone pairs are suitably oriented for a transition state involving equal binding of the two nitrogens to a single metal center, the process is intramolecular and fast at ambient temperature.[4] Moreover, in the solid state we found significant distortions from planar coordination, with N(1) displaced in a direction suggestive of the intramolecular transition state.[5,14] These displacements were correlated with the rate of the intramolecular processes in solution. In crystals of the phthalazine complex no significant displacement was found[6] and the solution-exchange process involved dissociative M–N bond cleavage.[4]

The structural evidence now at hand for the (3,5-dimethylpyrazole)palladium complex shows that although N(1) is out of the coordination plane, it lies on the same side of that plane as N(2), a distortion discussed above in terms of hydrogen bonding and not in any way suggestive of intramolecular metal–N(2) interaction. Thus the presence of the proton on N(2) prevents direct comparison with the previous results and represents a key difference in both the structural and mechanistic studies.

(25) Chenon, M. T.; Coupry, C.; Grant, D. M.; Pugmire, R. J. *J. Org. Chem.* **1977**, *42*, 659 and references therein.
(26) Litchman, W. M. *J. Am. Chem. Soc.* **1979**, *101*, 545.

Experimental Section

Data relating to the characterization of the complexes are given in the Results. Microanalyses were by D. L. McGillivray of this department.[13] In general the compounds tended to decompose on heating and melting points are not an especially useful method of characterization. IR spectra were recorded from 4000 to 200 cm^{-1} with accuracy ±3 cm^{-1} on a Perkin-Elmer Model 283 spectrophotometer. Solid samples were examined as Nujol mulls between cesium iodide plates. ^{31}P NMR spectra were recorded at 24.288 MHz on a Nicolet TT14 Fourier transform spectrometer using $P(OMe)_3$ as external reference. A total of 8192 data points was used in a 6000-Hz sweep, giving resolution of 1.46 Hz, and the ^{31}P parameters are thus subject to errors of this magnitude. ^1H NMR spectra were recorded at 90 MHz on a Perkin-Elmer R32 spectrometer using $Si(CH_3)_4$ as internal reference. In all NMR spectra *positive* chemical shifts are *downfield* from the reference.

Tetrafluoroborate and perchlorate salts of the cations $[M_2Cl_2(PEt_3)_4]^{2+}$, M = Pt or Pd, were prepared as previously described[12,27] as were the ligands 3,5-dimethylpyrazole[28] and 3,4,5-trimethylpyrazole.[29] Pyrazole (Aldrich Chemical Co.) and 4-bromo-3,5-dimethylpyrazole (PCR Research Chemicals) were commercially available.

The complexes $[PdCl(PEt_3)_2(pzH)]ClO_4$, $[PdCl(PEt_3)_2(3,5\text{-}DMP)]BF_4$, $[PdCl(PEt_3)_2(3,4,5\text{-}TMP)]BF_4$, $[PdCl(PEt_3)_2(Br\text{-}3,5\text{-}DMP)]ClO_4$, $[PtCl(PEt_3)_2(pzH)]ClO_4$, $[PtCl(PEt_3)_2(3,5\text{-}DMP)]ClO_4$, and $[PtCl(PEt_3)_2(3,4,5\text{-}TMP)]ClO_4$ were all prepared in high yield by cleavage of the appropriate $[M_2Cl_2(PEt_3)_4]^{2+}$ salt by the appropriate ligand under mild conditions in reactions similar to the following example.

***cis*-[PdCl(PEt$_3$)$_2$(3,5-DMP)][BF$_4$].** 3,5-Dimethylpyrazole (0.022 g, 0.23 mmol) in acetone (5 mL) was added dropwise to a stirred solution of $[Pd_2Cl_2(PEt_3)_4][BF_4]_2$ (0.11 g, 0.12 mmol) in acetone (10 mL). The yellow color of the dimer was rapidly discharged, and after being stirred for 20 min the solution was concentrated under reduced pressure to 3 mL. Diethyl ether (1.5 mL) was added and the solution cooled to −25 °C to yield the complex as colorless crystals (0.096 g, 0.17 mmol, 71%).

Crystals suitable for study by X-ray diffraction were grown by slow diffusion of diethyl ether into a dichloromethane solution of the complex.

Crystal Measurements. Preliminary oscillation, Weissenberg, and precession photographs were taken with Cu Kα radiation. The crystal data are given in Table I. The Delaunay reduced cell was used. The density of the crystal was measured by flotation in a solution of carbon tetrachloride and ether. The preliminary unit cell was refined by the method of least squares using 36 pairs of 2θ measurements obtained on a Picker four-circle diffractometer with automatic centering routines. These measurements were in the range 2θ = 24–45° with Mo Kᾱ radiation, λ = 0.710 69 Å. The Picker diffractometer was used for all the intensity measurements and was driven by a PDP-11/10 computer using locally written programs. The crystal was mounted on the *c* axis. The measurements were complete to 2θ = 50° in one hemisphere ($h \geq 0$). For each reflection the $\theta/2\theta$ scan consisted of 50 steps of 0.04° in 2θ, counting for 1 s at each step. Background measurements were for 25.0 s at each end of the motion. Three standards 400, 050, and 004 were measured at intervals of 50 reflections and used to evaluate an instrument instability constant (0.049). Only those measurements for which $I/\sigma(I) > 3$, based on counting statistics, were included in the diffractometer output. Lorentz, polarization, and instrument variation factors were applied. Corrections for absorption were carried out by using Gaussian quadrature with a 6 × 6 × 6 grid. The crystal shape is specified by the perpendicular distances of six faces from a central origin: {100}, 0.176 mm; {010}, 0.0845 mm; {001}, 0.156 mm. The range of transmissions was 0.77–0.86. After sorting and merging, there were 3038 independent reflections in the file of measurements.

Crystal Structure Solution and Refinement. The structure was solved by use of the Patterson function and the heavy-atom method. The programs used were supplied by Penfold[30] and are based on ORFLS, FORDAP, ORTEP, and ORFFE. The atomic scattering factors used were for uncharged atoms.[31] The *R* value was 0.368 with Pd only. The lighter atoms were found by the use of difference syntheses. The refinement was by full-matrix least-squares minimizing $\sum w(|F_o| - |F_c|)^2$, and convergence was attained for the nonhydrogen atoms after six cycles. The hydrogen atoms of the triethylphosphine ligands were then added at calculated positions (C–H = 0.97 Å) while the pyrazole hydrogen atoms were located by means of difference maps. The final SFLS cycle gave $R = 0.044$ and $R_w = 0.054$ where $R_w = (\sum w\Delta^2/\sum wF_o^2)^{1/2}$, the weights being derived from the instrument instability constant and the counting statistics. An analysis of $\sum w\Delta^2$ for sets of reflections chosen according to $(\sin\theta)/\lambda$ and $|F_o|$ showed no serious trends. No significant peaks were found in the final difference map, the maximum being 0.51 e Å^{-3} and $\sigma(\rho)$ = 0.11 e Å^{-3}. The final atomic parameters are given in Table II.

Registry No. *cis*-$[PdCl(PEt_3)_2(3,5\text{-}DMP)]BF_4$, 76648-91-4; *cis*-$[PdCl(PEt_3)_2(Br\text{-}3,5\text{-}DMP)]ClO_4$, 76648-93-6; *cis*-$[PdCl(PEt_3)_2(3,4,5\text{-}TMP)]BF_4$, 76648-95-8; *cis*-$[PdCl(PEt_3)_2(pzH)]ClO_4$, 76648-97-0; *cis*-$[PtCl(PEt_3)_2(3,5\text{-}DMP)]ClO_4$, 76665-43-5; *cis*-$[PtCl(PEt_3)_2(3,4,5\text{-}TMP)]ClO_4$, 76665-45-7; *cis*-$[PtCl(PEt_3)_2(pzH)]ClO_4$, 76665-47-9; $[Pd_2Cl_2(PEt_3)_4][BF_4]_2$, 22180-55-8; $[Pd_2Cl_2(PEt_3)_4][ClO_4]_2$, 76665-48-0; $[Pt_2Cl_2(PEt_3)_4][ClO_4]_2$, 52590-87-1; *trans*-$[PdCl(PEt_3)_2(Br\text{-}3,5\text{-}DMP)]^+$, 76704-55-7.

Supplementary Material Available: Tables of analytical data, fractional atomic coordinates of H atoms, and structure factor amplitudes (12 pages). Ordering information is given on any current masthead page.

(27) Dixon, K. R.; Hawke, D. J. *Can. J. Chem.* **1971**, *49*, 3252.
(28) *Beilstein, 4th ed.* **1936**, *H23*, 74.
(29) Rothenburg, R. v. *J. Prakt. Chem.* **1895**, [2] *52*, 45.
(30) Penfold, B. R. University of Canterbury Crystallographic Programs, Christchurch, New Zealand.
(31) Cromer, D. T.; Waber, J. T. "International Tables for X-ray Crystallography"; Kynoch Press: Bimingham, England, 1974; Vol. IV, Table 2.2B, 99.